RESEARCH PAPER

TM-25659 enhances osteogenic differentiation and suppresses adipogenic differentiation by modulating the transcriptional co-activator TAZ

EJ Jang[1†], H Jeong[1†], JO Kang[1], NJ Kim[2], MS Kim[2], SH Choi[2], SE Yoo[2], JH Hong[3], MA Bae[2] and ES Hwang[1]

[1]College of Pharmacy and Division of Life and Pharmaceutical Sciences and Center for Cell Signaling and Drug Discovery Research, Ewha Womans University, Seoul Korea, [2]Korea Research Institute of Chemical Technology, Daejeon, Korea, and [3]School of Life Science and Biotechnology, Korea University, Anam-dong, Seongbuk-gu, Seoul, Korea

BACKGROUND AND PURPOSE

The transcriptional co-activator with PDZ-binding motif (TAZ) is characterized as a transcriptional modulator of mesenchymal stem cell differentiation into osteoblasts and adipocytes. Moreover, increased TAZ activity in the nucleus enhances osteoblast differentiation and suppresses adipocyte development by interacting with runt-related transcription factor 2 (RUNX2) and PPARγ, respectively. Therefore, it would be of interest to identify low MW compounds that modulate nuclear TAZ activity.

EXPERIMENTAL APPROACH

High-throughput screening was performed using a library of low MW compounds in order to identify TAZ modulators that enhance nuclear TAZ localization. The effects and molecular mechanisms of a TAZ modulator have been characterized in osteoblast and adipocyte differentiation.

KEY RESULTS

We identified 2-butyl-5-methyl-6-(pyridine-3-yl)-3-[2′-(1H-tetrazole-5-yl)-biphenyl-4-ylmethyl]-3H-imidazo[4,5-b]pyridine] (TM-25659) as a TAZ modulator. TM-25659 enhanced nuclear TAZ localization in a dose-dependent manner and attenuated PPARγ-mediated adipocyte differentiation by facilitating PPARγ suppression activity of TAZ. In addition, TAZ-induced RUNX2 activity activation was further increased in osteoblasts, causing increased osteoblast differentiation. Accordingly, TM-25659 suppressed bone loss *in vivo* and decreased weight gain in an obesity model. After oral administration, TM-25659 had a favourable pharmacokinetic profile.

CONCLUSION AND IMPLICATIONS

TM-25659 stimulated nuclear TAZ localization and thus caused TAZ to suppress PPARγ-dependent adipogenesis and enhance RUNX2-induced osteoblast differentiation *in vitro* and *in vivo*. Our data suggest that TM-25659 could be beneficial in the control of obesity and bone loss.

Abbreviations

C/EBP, CCAAT-enhancer binding protein; DMSO, dimethyl sulphoxide; micro-CT, micro-computed tomography; MSC, mesenchymal stem cell; PEG, polyethylene glycol; PPRE, PPARγ-responsive element; RAR, retinoid acid receptor; RBE, RUNX2-binding element; RT, reverse transcription; RUNX2, runt-related transcription factor 2; TAZ, transcriptional coactivator containing PDZ-binding motif; TBX, T-box transcription factor; TM-25659, 2-butyl-5-methyl-6-(pyridine-3-yl)-3-[2′-(1H-tetrazole-5-yl)-biphenyl-4-ylmethyl]-3H-imidazo[4,5-b]pyridine]; TTF-1, thyroid transcription factor-1; WWTR1, WW domain-containing transcriptional co-regulator

Introduction

The protein transcriptional co-activator with PDZ-binding motif (TAZ), also referred to as WW domain-containing transcriptional co-regulator (WWTR1), was originally cloned as an interacting protein of the 14-3-3 protein that is involved in the control of cell cycle progression, cell differentiation and apoptosis through interaction with phosphorylated signalling molecules (Fu *et al.*, 2000). Based on biochemical analysis, TAZ contains multiple protein–protein interaction domains such as WW and coiled-coil domains, as well as a PDZ-binding motif (Lu *et al.*, 1999; Bedford *et al.*, 2000; Kanai *et al.*, 2000). As phosphorylation of TAZ at Ser[89] is a prerequisite for binding to the 14-3-3 protein and cytosolic localization (Kanai *et al.*, 2000), mutation of this residue in TAZ diminishes its interaction with the 14-3-3 protein and suppresses 14-3-3-mediated nuclear export, resulting in an increased level of TAZ in the nucleus (Kanai *et al.*, 2000). It is likely that the increased level of nuclear TAZ subsequently enhances its association with a transcription factor that regulates its effect on target gene transcription.

A number of transcription factors, including runt-related transcription factor 2 (RUNX2) and PPARγ, have been identified as proteins that associate with TAZ in the nucleus via a Pro-Pro-X-Tyr motif (Kanai *et al.*, 2000; Park *et al.*, 2004; Murakami *et al.*, 2005; Lei *et al.*, 2008; Wang *et al.*, 2009). While genetic deletion of RUNX2 in mice results in severe bone formation defects (Komori *et al.*, 1997; Otto *et al.*, 1997), sustained RUNX2 activity induces osteoblast differentiation from mesenchymal stem cells (MSCs) (Harada and Rodan, 2003; Ito, 2004). Moreover, PPARγ is critical for the adipocyte lineage commitment of MSCs and fatty acid metabolism by promoting adipocyte-specific gene expression (Chawla *et al.*, 1994; Rosen *et al.*, 1999; Ross *et al.*, 2000). Recently, it was reported that TAZ modulates the activity of RUNX2 and PPARγ during the lineage commitment of MSCs (Hong *et al.*, 2005). TAZ associates with RUNX2 and intensifies RUNX2-mediated osteogenic gene transcription, whereas its interaction with PPARγ restrains PPARγ-induced adipogenic gene expression (Hong *et al.*, 2005). Subsequently, stabilized TAZ expression enhances osteoblast development and suppresses adipocyte differentiation. On the other hand, TAZ-deficient MSCs prefer adipocyte differentiation to osteoblasts, indicating a potential role of TAZ in bone and fat metabolism (Hong *et al.*, 2005; Hong and Yaffe, 2006). In addition, activity of the myogenic regulatory factor MyoD is controlled by TAZ through physical association during myogenic differentiation (Jeong *et al.*, 2010). TAZ also interacts with thyroid transcription factor-1 (TTF-1) and T-box transcription factor

(TBX)-5 and subsequently controls lung epithelial cell differentiation and cardiac development respectively (Park *et al.*, 2004; Murakami *et al.*, 2005). Therefore, persistent nuclear TAZ localization is likely to be important in the modulation of transcription factor activities during cell differentiation.

In this study, we sought to identify low MW compounds that could modulate TAZ, by screening a library of small molecules. We identified a compound, 2-butyl-5-methyl-6-(pyridine-3-yl)-3-[2′-(1H-tetrazole-5-yl)-biphenyl-4-yl-methyl]-3H-imidazo[4,5-b]pyridine (TM-25659) that enhanced TAZ expression in the nucleus. Interestingly, TM-25659 treatment also enhanced RUNX2-induced osteoblast differentiation but suppressed PPARγ-mediated adipocyte differentiation in a TAZ-dependent manner. Moreover, *in vivo* treatment with TM-25659 attenuated both weight gain and bone loss in rats.

Methods

Animals

All animal care and experimental protocols were in accordance with IACUC guidelines and were approved by the IACUC committee at Ewha Womans University (IACUC 2010–23-3). C57BL/6 (B6) wild-type (WT) and TallyHo/JngJ (TH) mice were obtained from Jackson Laboratory (Bar Harbor, ME, USA). Male Sprague-Dawley rats were purchased from Orient Bio Inc. (Seongnam, Korea) and housed in the specific pathogen-free animal facility of Ewha Womans University.

Measurement of body weight and bone mineral density (BMD)

About 4- to 6-week-old mice were divided into two groups of six mice. Mice were provided a standard chow diet or a high-fat diet (HFD) with 60% kcal from fat (Harlan Teklad, Madison, WI, USA) *ad libitum* for 9 weeks. Their body weight was measured weekly. Mice were injected with either vehicle or TM-25659 every other day for 2 weeks before killing and the body weight was assessed before each injection. After 8 weeks, each animal was anaesthetized and imaged on a live-animal micro-computed tomography (micro-CT) scanner (eXplore Locus, GE Healthcare Biosciences, London, ON, Canada). BMD was evaluated in the femoral bones according to the manufacturer's instructions (GE Healthcare).

Cell culture

Preadipocyte 3T3-L1 (CL-173), osteoblast MC3T3-E1 (CRL-2593), murine MSCs C3H10T1/2 (CCL 226), COS-7 cells

(CRL-1651) and HEK 293T cells (CRL-1573) were purchased from the American Type Culture Collection (Manassas, VA, USA) and cultured in Dulbecco's modified Eagle's medium (Invitrogen, Carlsbad, CA, USA). Mouse embryonic fibroblasts (MEFs) were constructed from WT and TAZ knockout (KO) mouse embryos as previously described (Hong et al., 2005).

High-throughput screening

COS-7 cells were seeded into a 96-well plate and transfected with green fluorescence protein-tagged TAZ expression vector (GFP-TAZ) and red fluorescence protein-tagged histone 2B (RFP-H2B) expression vector. Cells in each well were then incubated with 10 μM of a compound from the chemical library for 2 h. DMSO was added to the cells as a control. The cells were photographed using a BD Pathway high-throughput cell-imaging platform and the relative nuclear localization of TAZ was calculated by normalization to RFP-H2B according to the manufacturer's handbook (Becton Dickinson Biosciences, San Jose, CA, USA).

Adipogenic and osteogenic cell differentiation

3T3-L1 pre-adipocytes were plated and cultured for 48 h to achieve 100% confluency and then replaced with adipogenic differentiation medium (5 μg·mL^{-1} of insulin, 1 μM dexamethasone, and 2 μM rosiglitazone). Cells were replaced with insulin medium after 48 h and then induced to differentiate for 6 days. Cells were fixed with 10% formalin and stained with 0.3% oil red O solution. Dyes were eluted in 100% isopropanol with gentle shaking and then assayed by spectrometry at 500 nm for quantitation. For adipogenic transdifferentiation, MEFs and C3H10T1/2 MSCs were infected with viruses expressing PPARγ and cultured in adipogenic differentiation medium for 6 days. Separately, osteoblast differentiation was induced in MC3T3-E1 and C3H10T1/2 cells for 6 and 14 days, respectively, under osteogenic differentiation conditions containing β-glycerophosphate (10 mM) and ascorbic acid (50 μg·mL^{-1}). Osteoblasts were fixed with 70% ethanol and stained with 2% (w/v) alizarin red S solution (pH 4.3) to detect calcified matrix (an early indicator of mineralized matrix deposition). For quantification, the dye was dissolved in 10% w/v cetylpyridinium chloride (in 10 mM sodium phosphate, pH 7.0; Sigma-Aldrich) and subsequently analysed by spectrometry (405 nm). Alkaline phosphatase (ALP) activity was assayed using an ALP Colorimetric Assay Kit according to the manufacturer's instruction (ABcam, Cambridge, MA, USA).

Reverse transcription (RT) and real-time PCR analysis

RT was performed using 2 μg of total RNA in a final reaction volume of 20 μL using a Superscript II RT kit (Invitrogen). For quantitative real-time PCR reaction, the RT reaction mixture was assayed with a SYBR Green pre-mix buffer and gene-specific primers using an ABI-Prism 7700 sequence detector (Perkin-Elmer Applied Biosystems, Foster City, CA, USA). Specific primers were as follows: PPARγ 5′-ccttgctgtgggg atgtctca-3′, 5′-ctccttctcgg cctgtggcat-3′; TAZ 5′-gtcaccaacagtag ctcagatc-3′, 5′-agtgattacagccaggttagaaag-3′; aP2 5′-gtgggaacct ggaagcttgtc-3′, 5′-cttcaccttcctgtcgtctgc-3′; adiponectin 5′-gat

ggcagagatggcactcc-3′, 5′-cttgccagtgctgccgtcat-3′; RUNX2 5′-ctcagtgatttagggcgcatt-3′, 5′-aggggtaagactggtcatagg-3′; osteocalcin 5′-ctagcagacaccatgaggac-3′, 5′-caggtcctaaatagtgatacc-3′; ALP 5′-atggtaacgggcctggctaca-3′, 5′-agttctgctcatggacgccgt-3′; osterix 5′-tggcgtcctctctgcttga-3′, 5′-tcagtgagggaagggtgggt-3′; and β-actin 5′-aagcaggagtatgacgagtccg-3′, 5′-cggaactaagtca tagtccgcg-3′. Relative transcript level was calculated by normalizing the threshold cycle (Ct) value to the β-actin level.

DNA pull-down assay

293T cells were transiently transfected with expression vectors for RUNX2, PPARγ and TAZ and then lysed with HKMG buffer (compostition: 10 mM HEPES, pH 7.9, 100 mM KCl, 5 mM MgCl$_2$, 10% glycerol, 0.1% NP-40, and 1 mM dithiothreitol). Whole cell extracts were incubated with biotinylated double stranded DNA for 1 h, followed by incubation with streptavidin agarose beads. Precipitates were washed with HKMG buffer and resolved by SDS-PAGE followed by immunoblot assay. Double-stranded DNA sequences for PPARγ-responsive element (PPRE) and RUNX2-binding site (RBE) were 5′-caaaactaggtcaaag-3′ and 5′-ctagaactgaccgcag-3′ respectively.

Reporter gene assay

Cells were transfected with expression vector for RUNX2, PPARγ or TAZ together with either 6xOSE-luc or aP2-luc as a reporter gene. Cells were subsequently incubated with TM-25659 for 24 h before harvesting. Relative luciferase activity was measured according to the manufacturer's protocol (Promega, Madison, WI, USA). pCMVβ reporter gene was co-transfected into the cells, and β-galactosidase activity was assayed for transfection efficiency normalization (TROPIX, Bedford, MA, USA).

In vitro interaction assay

293T cells were transiently transfected with Flag-tagged TAZ and RUNX2 expression vector, followed by 24 h TM-25659 treatment. Immune complexes were obtained by incubating whole cell extracts with Flag-M2 agarose beads (Sigma-Aldrich), followed by SDS-PAGE and immunoblot analysis.

In vivo pharmacokinetic study of TM-25659 in rats

Adult male Sprague-Dawley rats were anaesthetized with an injection of ketamine (125 mg kg^{-1}, i.m.; Yuhan Corp., Korea) and the jugular and femoral veins were cannulated with polyethylene tubing (PE-50; BD Intramedic, Clay Adams, USA). Rats were allowed to recover from anaesthesia for 1 day before the study. The cannula was flushed with heparinized saline (20 U·mL^{-1}) to prevent blood clots. Rats were given TM-25659 (in DMSO/PEG400/distilled water, 0.5:4:5.5, v/v) either by i.v injection (2 mL kg^{-1}) or by mouth (gavage, 2 mL kg^{-1}) to provide a dose of 10 mg·kg^{-1}. Blood samples were collected (with heparin) at predetermined time points; 2, 10 and 30 min, and 1, 2, 4 and 8 h after i.v. injection; and 15 and 30 min, and 1, 2, 4 and 8 h after oral administration. The urine samples collected from the rats, in metabolic cages over 24hr, were pooled and analysed by LC/MS/MS analysis as reported (Kim et al., 2011).
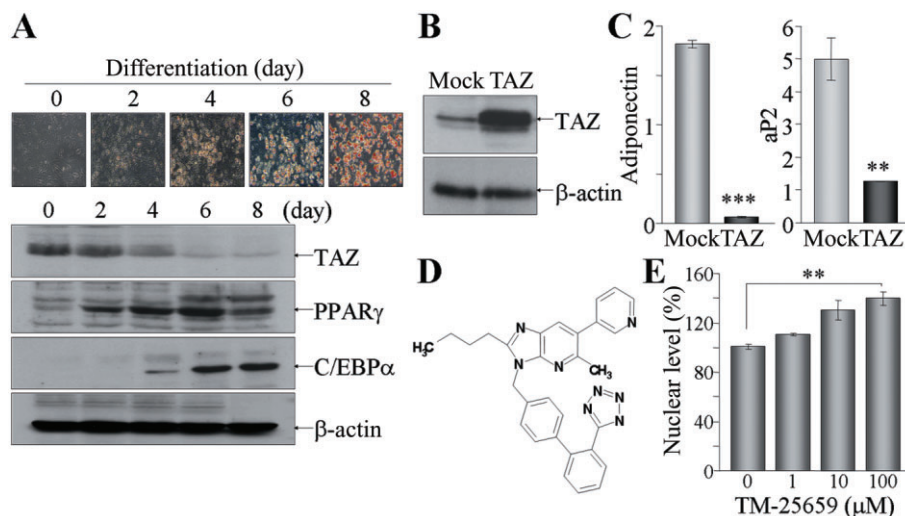
Figure 1

TM-25659, a novel modulator of TAZ. (A) 3T3-L1 cells were grown to confluency and induced to differentiate under adipogenic differentiation conditions. Cells were harvested at the indicated time points, followed by oil red O staining and immunoblot analysis with antibodies against TAZ, PPARγ or C/EBPα. (B and C) TAZ stable cell line was constructed in 3T3-L1 cells by viral infection. TAZ expression was analysed by immunoblot analysis (B). The cell lines were differentiated into adipocytes for 6 days and subjected to RT and real-time PCR (C). (D) Chemical structure of TM-25659. (E) Cos-7 cells transfected with GFP-TAZ and RFP-H2B were treated with the indicated amounts of TM-25659 and quantitative nuclear intensities of TAZ were calculated using a BD Pathway HT cell-imaging platform and Bioimager software. Nuclear levels of TAZ in vehicle-treated cells was set as 100%. **$P < 0.005$.

Statistical analysis

Most experimental results are expressed as mean ± SEM of at least 3 independent experiments and were assessed by one-way ANOVA and unpaired Student's *t*-test. *P*-values < 0.05 were considered statistically significant.

Materials

All reagents required for osteoblast and adipocyte differentiation and cell staining were purchased from Sigma-Aldrich Corp. (St. Louis, MO, USA). A library of low MW compounds was generated by individual synthesis to 95% purity at the Korean Research Institute of Chemical Technology (KRICT). TM-25659 (MW = 500; pKa = 5.27; LogP = 6.97 ± 0.37) was synthesized at the KRICT to 98% purity by HPLC (Yoo *et al*., 1999). TM-25659 has a solubility of 134.3 ± 2.9 μM in water. For administration *in vivo*, TM-25659 was dissolved in dimethyl sulphoxide (DMSO)/polyethylene glycol (PEG) 400/distilled water (0.5:4:5.5, v/v).

Results

TM-25659 modulates expression of TAZ, an endogenous suppressor of adipogenesis

TAZ functions as a suppressor of adipocyte differentiation by inhibiting PPARγ activity in the nucleus because TAZ deficiency enhanced adipocyte differentiation of 3T3-L1 pre-adipocytes and MSCs (Hong *et al*., 2005). We induced differentiation of 3T3-L1 pre-adipocytes into mature adipocytes by adding adipogenic inducers, such as insulin, and a PPARγ ligand, rosiglitazone (Ross *et al*., 2000), and found that

TAZ expression decreased in a time-dependent manner during adipogenic differentiation while two adipogenic markers PPARγ and CCAAT-enhancer binding protein α (C/EBPα) increased (Figure 1A). Exogenous overexpression of TAZ in 3T3-L1 cells diminished adipocyte differentiation, which was shown by decreased levels of adiponectin and aP2 (Figure 1B and C). These results prompted us to search for low MW compounds that could increase TAZ expression and activity and thereby attenuate adipocyte accumulation. From library screening using COS-7 cells expressing GFP-tagged TAZ, we identified a low MW compound that modulated TAZ, TM-25659 (Figure 1D). Treatment of the cells with TM-25659 for 30 min increased GFP-TAZ intensities in a dose-dependent manner, as confirmed with a BD Pathway high-throughput bioimager in real time (Figure 1E).

TM-25659 promotes nuclear localization of TAZ proteins

As exogenous TAZ was apparently increased in the nucleus after treatment with TM-25659, we analysed the effect of TM-25659 on endogenous TAZ expression and nuclear localization by immunoblotting. The total amount of endogenous TAZ expression was not affected by treatment with TM-25659 in C3H10T1/2 cells (Figure 2A). However, fractionation of subcellular proteins and subsequent immunoblot analysis showed that the nuclear level of endogenous TAZ was increased by TM-25659 (Figure 2B) and this increase was confirmed by immunofluorescence staining with anti-TAZ antibody (Figure 2C). As dephosphorylation of Ser[89] in TAZ enhances nuclear TAZ localization (Kanai *et al*., 2000), we assessed serine phosphorylation of TAZ (Figure 2D). Treat-
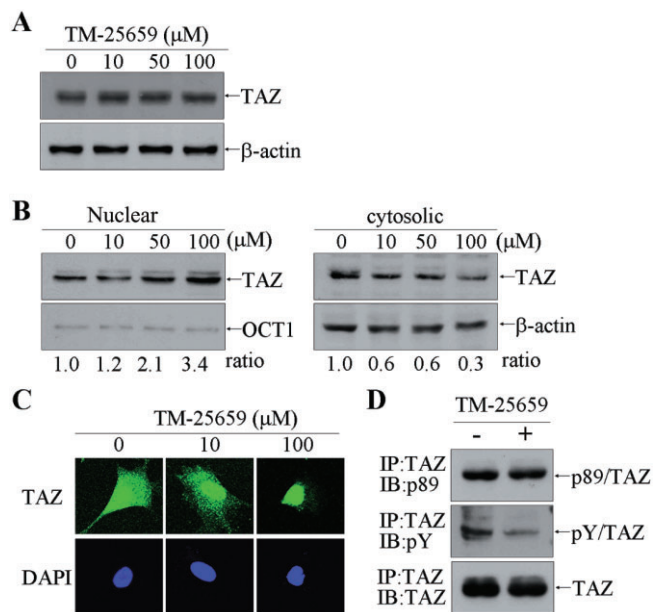
Figure 2

Nuclear localization of TAZ was enhanced by TM-25659. (A) C3H10T1/2 MSCs were treated with TM-25659 for 2 h. Whole cell extracts were resolved by SDS-PAGE and subsequently incubated with anti-TAZ antibody. (B) Nuclear and cytosolic proteins were prepared using the NE-PER kit (Pierce, Rockford, IL, USA) and 10 μg of nuclear protein and 50 μg of cytosolic proteins were used for SDS-PAGE and immunoblot analysis. OCT1 and β-actin were used as nuclear and cytosolic protein control respectively. (C) 3T3-L1 cells were treated with TM-25659 for 2 h and fixed for immunofluorescence assay using anti-TAZ antibody and Alexa 488-conjugated anti-rabbit IgG, followed by confocal microscopy. (D) 3T3-L1 cells were incubated with 100 μM TM-25659 for 2 h. TAZ protein was precipitated by incubation with anti-TAZ antibody and subjected to SDS-PAGE and immunoblotting with anti-pS89 TAZ antibody, phosphotyrosine antibody and anti-TAZ antibody.

ment with TM-25659 did not affect serine phosphorylation of TAZ, whereas tyrosine phosphorylation of this protein was decreased.

TM-25659 suppresses PPARγ-mediated adipocyte differentiation

Given that TM-25659 increased nuclear TAZ expression, we next investigated its effects on TAZ function in adipocyte differentiation. In 3T3-L1 cells, TM-25659 treatment significantly suppressed the normal adipocyte differentiation and lipid droplet formation (Figure 3A and B). As a result of attenuated adipogenic differentiation by TM-25659, the increased levels of PPARγ in differentiated adipocytes were decreased by TM-25659 in a concentration-dependent manner, whereas TAZ expression was substantially elevated (Figure 3C). In addition, the adipogenic marker aP2 and adiponectin expression were further decreased by TM-25659 (Figure 3D). These results demonstrate that TM-25659 acted as a suppressor of PPARγ-dependent adipocyte differentiation.
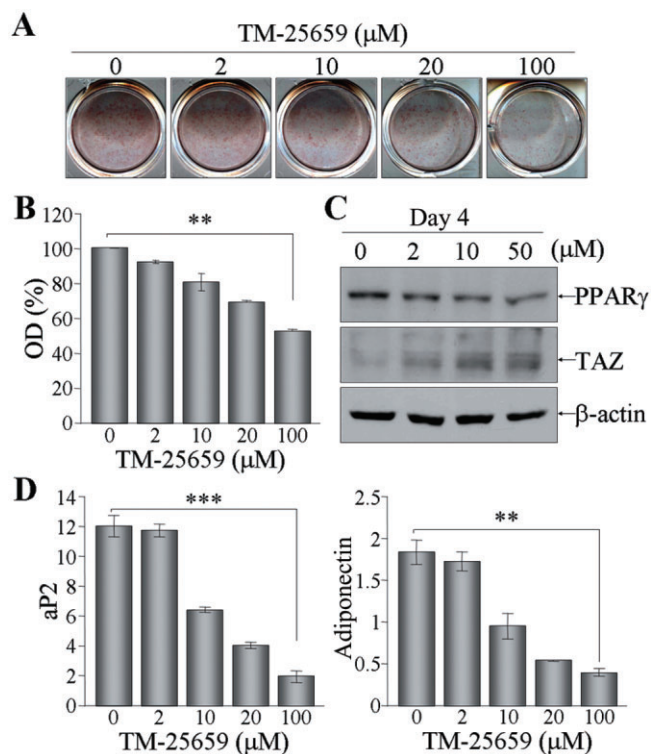

Figure 3

Suppression of adipocyte differentiation by TM-25659. 3T3-L1 cells were differentiated into adipocytes in the presence of indicated amounts of TM-25659. At 6 days post-differentiation, cells were stained with oil red O solution (A). Dyes were dissolved in methanol and analysed by measuring the OD at 500 nm (B).; **$P < 0.005$. (C) Cellular proteins were harvested at day 4 after differentiation, followed by SDS-PAGE and immunoblot analysis using anti-PPARγ or anti-TAZ antibody. (D) Total RNA was prepared from the cells after differentiation for 6 days and relative expression level of aP2 and adiponectin was determined after normalization to the level of β-actin.

TM-25659 enhances PPARγ suppression activity of TAZ in adipocyte differentiation

In order to uncover the inhibitory mechanisms of TM-25659 in adipogenesis, we examined the direct effect of TM-25659 on PPARγ expression and activity. The mRNA level of PPARγ was not changed by TM-25659 treatment for 24 h (Figure 4A). However, DNA-binding activity of exogenous PPARγ was substantially decreased by TM-25659 but only in the presence of TAZ (Figure 4B). These results indicated that TM-25659 inhibited DNA binding of PPARγ to its target gene promoter but did not affect PPARγ expression level. We next tested the TAZ dependency of TM-25659 for suppression of PPARγ activity, using a reporter assay with an aP2 promoter luciferase gene. PPARγ expression alone increased aP2 promoter activity by four to fivefold. The PPARγ-induced aP2 promoter activity was attenuated by TAZ co-expression but was not affected by addition of TM-25659. However, suppression of PPARγ activity by TAZ was facilitated in the presence of TM-25659, suggesting that TM-25659 requires TAZ expression, in order to suppress PPARγ activity (Figure 4C). Further
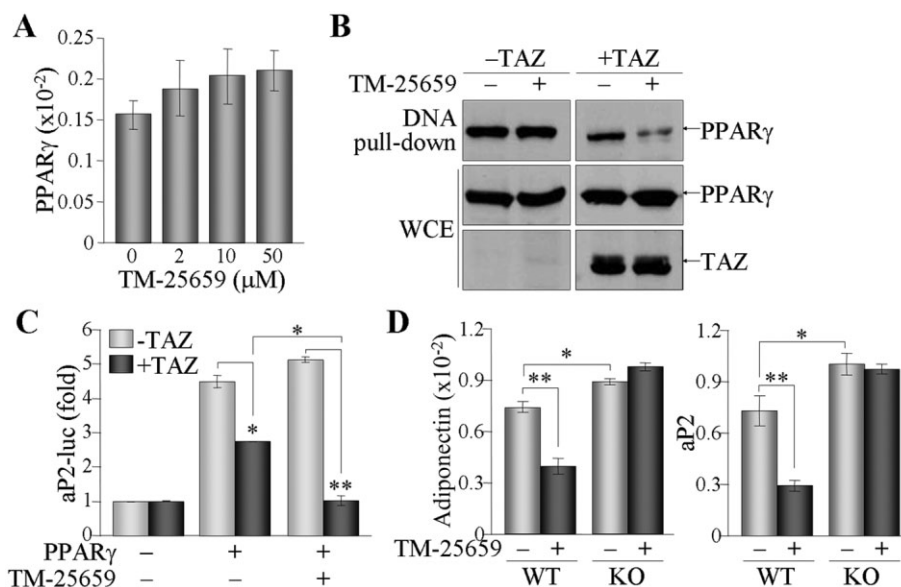
Figure 4

TAZ-dependent PPARγ suppression of TM-25659. (A) 3T3-L1 cells were treated with TM-25659 for 24 h. Total RNA was prepared using TRIzol and used for measurement of PPARγ mRNA level. (B) 293T cells were transiently transfected with PPARγ expression vector together with TAZ expression vectors and subsequently treated with TM-25659 (50 μM) for 24 h. Whole cell extracts were incubated with biotinylated PPRE sequence and subjected to precipitation with streptavidin agarose beads, followed by SDS-PAGE and blotting with anti-PPARγ or anti-TAZ antibody. (C) 293T cells were transfected with reporter genes (aP2-luc and pCMVβ) and expression vectors for PPARγ and/or TAZ and subsequently treated with TM-25659 (50 μM) for 24 h. Relative reporter activity was expressed as a fold induction after normalization with β-galactosidase activity. *$P < 0.05$; **$P < 0.005$. (D) TAZ WT and KO MEF cells were infected with PPARγ-expressing viral supernatants and were then cultured under adipogenic differentiation conditions with an additional presence of TM-25659 (10 μM) for 6 days. Total RNA was prepared for analysing mRNA levels of adiponectin and aP2.

evidence for TAZ-dependent TM-25659 action in adipogenic differentiation was provided by PPARγ-driven transdifferentiation of TAZ WT and KO MEFs into adipocytes. Both WT and TAZ KO MEFs were infected with PPARγ-expressing viruses and were induced to differentiate into adipocytes. In WT MEFs, the induced expression of adiponectin and aP2 was moderately but significantly decreased by TM-25659, whereas TM-25659 failed to suppress PPARγ-induced expression of aP2 and adiponectin in cells lacking TAZ (TAZ KO MEFs) (Figure 4D).

TAZ stimulates RUNX2-induced osteoblast development

As TAZ also modulates osteoblast differentiation, we assessed the effects of TM-25659 on osteoblast differentiation. TM-25659 substantially accelerated osteoblast differentiation of C3H10T1/2 cells and mineralization in a dose-dependent manner, as shown by Alizarin red S staining and quantitative analysis (Figure 5A and B). Moreover, the expression levels of osteogenic markers, such as osteocalcin, ALP and osterix were significantly increased by treatment with TM-25659, even at a concentration of 2 μM (Figure 5C). Treatment of MC3T3-E1 cells with TM-25659 during osteoblast differentiation also significantly elevated ALP activity (Figure 5D). Interestingly, TM-25659 enhanced osteogenic gene expression and thereby increased osteoblast differentiation.

TM-25659 augments TAZ activity to induce RUNX2-mediated osteogenic gene expression

Enhancement of osteogenic differentiation by TM-25659 prompted us to look for the underlying molecular mechanisms. We first examined RUNX2 expression in MC3T3-E1 cells and found that TM-25659 enhanced RUNX2 expression, thereby promoting osteoblast differentiation (Figure 6A). Moreover, TM-25659 facilitated DNA-binding activity of RUNX2 in the presence of TAZ (Figure 6B) and a physical interaction between RUNX2 and TAZ (Figure 6C). As reported (Hong et al., 2005), RUNX2-mediated osteocalcin promoter activity was increased by TAZ expression. While TM-25659 did not influence promoter activity by RUNX2 expression alone, synergistic activation of RUNX2 and TAZ on promoter activity was further increased by TM-25659 treatment (Figure 6D). However in MEFs lacking TAZ (TAZ KO), RUNX2-mediated osteocalcin expression was not increased by TM-25659 (Figure 6E), supporting the TAZ-dependent function of TM-25659 for promoting osteogenic differentiation.

TM-25659 attenuates weight gain and bone loss in vivo

The potent effects of TM-25659 on adipocyte and osteoblast differentiation in vitro led us to assay the anti-adipogenic and osteogenic actions of TM-25659 in vivo. C57BL6 mice were fed a high fat diet (HFD) for 9 weeks and were injected i.p. with either vehicle or TM-25659, for 16 days before the end of
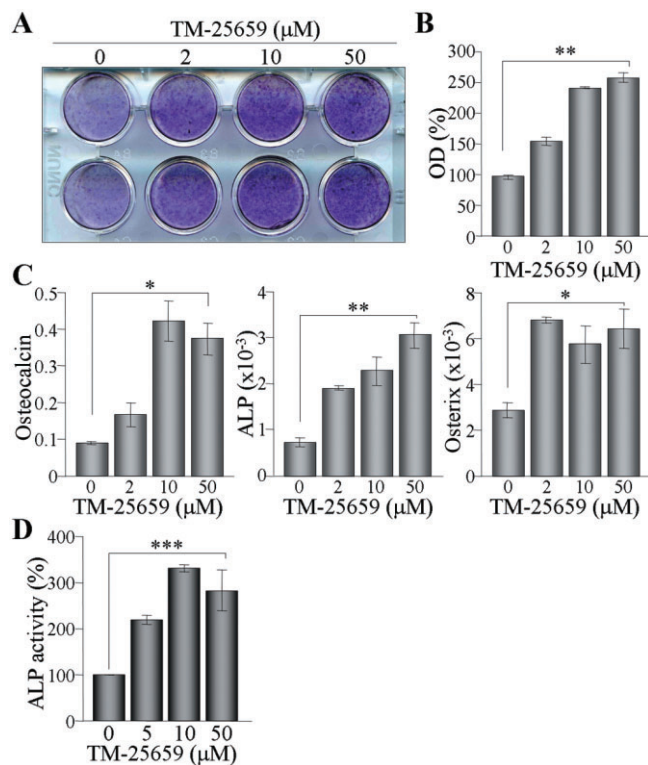
Figure 5

Stimulatory effect of TM-25659 on osteoblast differentiation and calcium deposition. (A) C3H10T1/2 cells were induced to differentiate into osteoblasts and cultured in the presence of TM-25659 for 14 days. Calcium deposition in osteoblasts was stained with Alizarin red S (A). Dyes were dissolved in cetylpyridinium chloride, and dye absorbance was measured by spectrophotometry (OD at 405 nm) (B). Total RNA was prepared from the cells and then analysed by RT and real-time PCR. Relative expression levels of osteocalcin, ALP and osterix were calculated after normalization to the level of β-actin (C). (D) MC3T3-E1 cells were induced to differentiate into osteoblasts for 6 days in the absence or presence of TM-25659. ALP activity was determined by measuring the absorbance at 405 nm. *$P < 0.05$; **$P < 0.005$; ***$P < 0.0005$.

the experiment. Body weight was increased by the HFD and this increase was substantially diminished in the TM-25659-treated group compared with the vehicle-treated group (Figure 7A). Moreover, TM-25659 treatment of *ob/ob* mice for 2 weeks consistently attenuated weight gain in these obese animals (Figure 7B). We studied the *in vivo* effects of TM-25659 on osteogenesis using an ovariectomy (OVX)-induced bone loss model. OVX rats displayed drastically diminished BMD because of oestrogen deficiency but also experienced increased weight gain and fat mass after OVX as expected (Chen and Heiman, 2001). Administration of alendronate, given as a positive control, had no effect on weight gain but prevented BMD loss in OVX rats (Figure 7C). Interestingly, oral administration of TM-25659 for 4 weeks moderately but significantly attenuated weight gain and partly restored BMD in the OVX rats (Figure 7C). Furthermore, in TallyHo/JngJ (TH) mice, a model of secondary osteoporosis

Table 1

Pharmacokinetic parameters of 2-butyl-5-methyl-6-(pyridine-3-yl)-3-[2′-(1H-tetrazole-5-yl)-biphenyl-4-ylmethyl]-3H-imidazo[4,5-b] pyridine] (TM-25659). TM-25659 was administered i.v. or p.o. to rats at a dose of 10 mg·kg⁻¹. Pharmacokinetic parameter values of TM-25659 were estimated using non-compartmental procedures

Pharmacokinetic parameters	i.v.	p.o.
T_{max} (h)	–	0.33 ± 0.14
C_{max} (µg·mL⁻¹)	–	3.34 ± 0.73
$t_{1/2}$ (h)	6.78 ± 1.95	9.85 ± 3.15
$AUC_{0 \to t}$ (µg·h·mL⁻¹)	43.72 ± 15.36	18.14 ± 3.89
$AUC_{0 \to \infty}$ (µg·h·mL⁻¹)	52.99 ± 23.58	23.29 ± 0.60
CL (L·h⁻¹·kg⁻¹)	0.21 ± 0.09	–
V_{ss} (L·kg⁻¹)	1.91 ± 0.03	–
MRT (h)	5.64 ± 1.74	7.57 ± 1.73
F_t (%)	–	41.50

Results are mean $\pm$ SD ($n = 6$). $AUC_{0 \to \infty}$, The integral of the plasma concentration (C_p) after administration; $AUC_{0 \to t}$, the area under time curve; CL, The volume of plasma cleared of the drug per unit time; C_{max}, the peak plasma concentration of a drug after oral administration; F, the fraction of drug absorbed; MRT, mean residence time; T_{max}, the time after administration of a drug when the maximum plasma concentration is reached; V_{ss}, the apparent volume in which a drug is distributed and reaches steady-state.

(Won *et al.*, 2011), oral TM-25659 (10 or 100 mg·kg⁻¹) increased BMD (Figure 7D).

TM-25659 may be an anti-adipogenic and an osteogenic drug with favourable pharmacokinetic profiles

TM-25659 exhibited potential to control adipocyte and osteoblast differentiation *in vitro* and *in vivo*. We thus investigated the pharmacokinetics of TM-25659 in rats. TM-25659 was given i.v. or p.o. to rats at a dose of 10 mg·kg⁻¹. The plasma concentration of TM-25659 was generally measurable at all times after dosing and declined with an approximate $t_{1/2}$ of 7 or 10 h following i.v or p.o. administration respectively (Figure 8 and Table 1). The systemic clearance (CL) was 0.21 L·h⁻¹·kg⁻¹ and the volume of distribution at steady-state (1.91 L·h⁻¹·kg⁻¹) was larger than the volume of total body fluids, indicating that TM-25659 may be well distributed to the tissues (Table 1). Other pharmacokinetic parameters shown in Table 1 demonstrated that TM-25659 had good oral bioavailability in rats.

Discussion and conclusions

In this study, we first identified TM-25659, as a low MW compound affecting the nuclear activity of TAZ, using a HT library screening system. We additionally confirmed the TAZ-dependent modulatory activity of TM-25659 in adipocyte
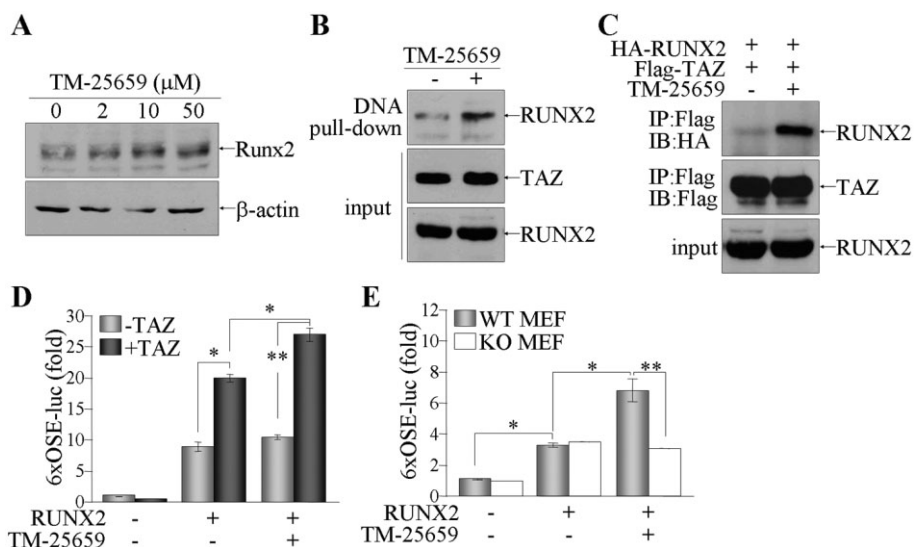
Figure 6

Enhancement of RUNX2 activity by TM-25659 depends on TAZ expression. (A) Confluent MC3T3-E1 cells were treated with TM-25659 for 48 h under osteoblast differentiation conditions. Nuclear proteins were harvested and analysed by SDS-PAGE and immunoblot of RUNX2. (B and C) 293T cells were transfected with both RUNX2 and Flag-tagged TAZ expression vectors, and treated with either vehicle or TM-25659 (50 μM) for 24 h. Cellular proteins were incubated with either Flag-M2 agarose beads (B) or biotinylated RBE DNA, followed by incubation with streptavidin agarose beads (C). Precipitates were resolved by SDS-PAGE and protein blots were incubated with antibodies against RUNX2 or TAZ. (D) 293T cells were transfected with RUNX2 and/or TAZ expression vector along with reporter genes (6xOSE-luc and pCMVβ), followed by treatment with TM-25659 (50 μM) for 24 h. (E) TAZ WT and KO MEF cells were transiently transfected with RUNX2 expression vector and reporter genes (6xOSE-luc and pCMVβ). Cells were treated with TM-25659 (50 μM) for 24 h and relative reporter activity was expressed as a fold induction after normalization with β-galactosidase activity. *$P < 0.05$; **$P < 0.005$.

and osteoblast differentiation as evidenced by loss of the anti-adipogenic and osteogenic activity of TM-25659 in TAZ-deficient cells. Thus, TM-25659 may play beneficial roles in the control of obesity and bone loss through activation of TAZ.

Although TM-25659 significantly increased nuclear localization of TAZ without changing the total amount of TAZ, the precise mechanism by which TM-25659 controls TAZ localization is not yet clearly characterized. TAZ undergoes phosphorylation at Ser[89] and specifically interacts with the 14-3-3 protein, restricting TAZ expression mostly in the cytosol (Kanai et al., 2000). However, serine phosphorylation of TAZ was not affected by treatment with TM-25659, but tyrosine phosphorylation of TAZ was reduced, suggesting a potential role of TM-25659 in modification-induced structural changes of TAZ. It is also likely that TM-25659 directly interacted with TAZ and modulated its nuclear localization. Many reports have found that the ligand binding to nuclear hormone receptors such as PPARα, PPARβ, PPARγ, retinoid acid receptor (RAR) and oestrogen receptor (ER) increased DNA-binding, dimerization and transcriptional activities (Jans, 1994; MacLean et al., 1997; Clevenger, 2003; Claessens and Gewirth, 2004; Smith and O'Malley, 2004). For example, binding of a selective oestrogen modulator, tamoxifen, to ERs induced conformational alterations, thus affecting the ability of ERs to interact with other proteins, such as co-activators and co-repressors and to modulate target gene transcription (Kuroda et al., 1985; Ray et al., 1994; Brzozowski et al., 1997; Shiau et al., 1998). Likewise, TM-25659 may directly bind to TAZ and promote conformational changes and subsequent

interaction with various transcription factors such as RUNX2 and PPARγ. Exactly how tyrosine phosphorylation and other structural changes of TAZ could be directly or indirectly induced by TM-25659 remains to be elucidated through protein purification and X-ray crystallography. Such analysis would explain how TM-25659 stimulates the nuclear localization of TAZ.

In addition to the regulatory control of TAZ in cell differentiation, it has been recently reported that TAZ promotes cell proliferation and epithelial-to-mesenchymal transition, and thus aggravates breast cancer and lung cancer (Lei et al., 2008; Chan et al., 2011; Lai et al., 2011; Zhou et al., 2011). Disruption of the TEAD-TAZ transcription complex or silencing of TEAD gene expression abolished TAZ-mediated tumour cell growth, suggesting an oncogenic potential of TAZ through TEAD activation in the Hippo pathway (Chan et al., 2008; 2009; Zhang et al., 2009). Although the hyperproliferation of tumour cells is induced by TAZ, it is not yet known if TAZ induction in normal cells induces tumour growth and progression or if TAZ deficiency blocks tumourigenesis in vivo. For the development of TM-25659 as a safe and effective medicine, it is clearly necessary to determine the effects of this compound on cell proliferation and tumour growth.

Our results demonstrated that TM-25659 exerted potent anti-adipogenic and osteogenic activities. The comprehensive molecular mechanism of TM-25659 action specifically entails TAZ-dependent regulation of cellular differentiation. Thus, TM-25659 may be beneficial for preventing and controlling chronic metabolic diseases such as obesity and osteoporosis. Alendronate is widely used for treating and preventing
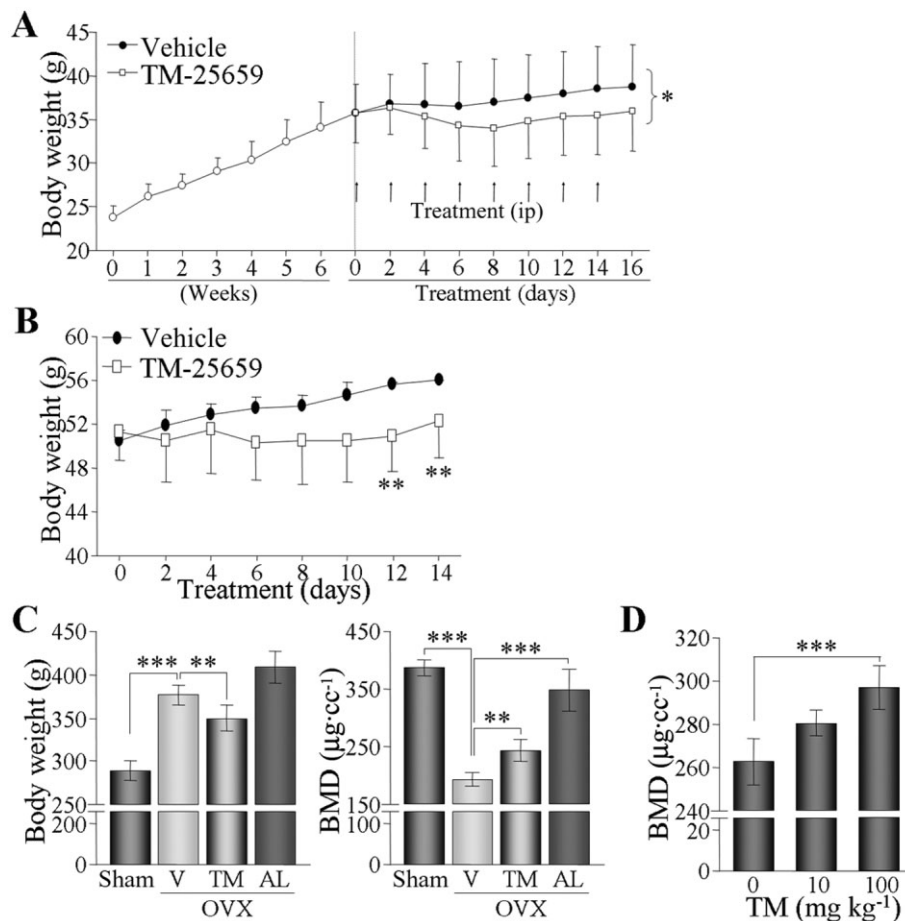
Figure 7

In vivo protective roles of TM-25659 against weight gain and bone loss. (A) B6 WT mice were fed HFD for 7 weeks, divided into two groups (*n* = 6 for each group) and then injected i.p. every other day with either vehicle or TM-25659 (50 mg·kg^{-1}) for 2 weeks. Body weight was measured and expressed as mean ± SEM of six mice. (B) Twelve-week-old *ob/ob* mice were given either vehicle or TM-25659 (50 mg·kg^{-1} i.p.) for 2 weeks (*n* = 6). Body weight was measured every 2 days. (C) Rats (*n* = 12) were ovariectomized (OVX) and then given oral vehicle (V), TM-25659 (TM) or alendronate (AL) every other day. AL was used as a positive control. All rats were then killed at 10 weeks after OVX. Body weight was measured and BMD was calculated using a micro-CT scanner. (D) Four-week-old osteoporotic male TH mice were given oral TM-25659 for 4 weeks. BMD was measured from each animal and expressed as mean ± SEM of six mice. *$P < 0.05$; **$P < 0.005$; ***$P < 0.0005$.
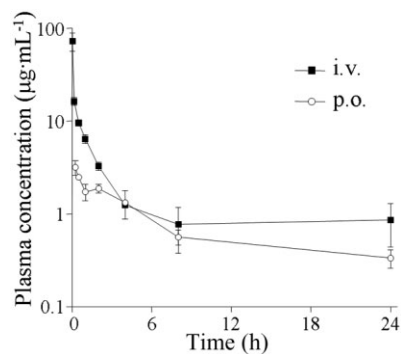

Figure 8

Plasma concentration-time profile of TM-25659. TM-25659 was administered i.v. or p.o. to rats at a dose of 10 mg·kg^{-1}. The plasma concentration of TM-25659 was measured at different time points and is presented as mean ± SD of six rats.

osteoporosis because it functions as a positive regulator in osteoblast generation and bone mineralization (Sahni *et al.*, 1993; Nishikawa *et al.*, 1996; Vitte *et al.*, 1996; Wang *et al.*, 2010) and an inhibitor of osteoclast formation and activity (Saag *et al.*, 1998; Orwoll *et al.*, 2000). Despite the promising effects of alendronate in osteoporosis, long-term administration of this compound for osteoporosis is accompanied by side effects such as oesophageal injury and osteonecrosis of the jaw (Wezeman *et al.*, 2000; Watts and Diab, 2010). The protection by TM-25659 against oestrogen deficiency-induced bone loss appeared to be less effective than that of alendronate, but TM-25659 offers an additional benefit by attenuating weight gain, a frequent finding in osteoporosis patients. Although extensive studies on the long-term bioavailability, efficacy, safety and side effects of TM-25659 are required for its development as an anti-osteoporotic and anti-adipogenic medication, our results suggest that TM-25659 may be an attractive new candidate for the development of a

new anti-osteoporotic and anti-obesity drug that acts by regulating endogenous TAZ activity for the modulation of adipocyte and osteoblast development.

Acknowledgements

Conflicts of interest

The authors state no conflict of interest.

References

Bedford MT, Sarbassova D, Xu J, Leder P, Yaffe MB (2000). A novel pro-Arg motif recognized by WW domains. J Biol Chem 275: 10359–10369.

Brzozowski AM, Pike AC, Dauter Z, Hubbard RE, Bonn T, Engstrom O et al. (1997). Molecular basis of agonism and antagonism in the oestrogen receptor. Nature 389: 753–758.

Chan SW, Lim CJ, Guo K, Ng CP, Lee I, Hunziker W et al. (2008). A role for TAZ in migration, invasion, and tumorigenesis of breast cancer cells. Cancer Res 68: 2592–2598.

Chan SW, Lim CJ, Loo LS, Chong YF, Huang C, Hong W (2009). TEADs mediate nuclear retention of TAZ to promote oncogenic transformation. J Biol Chem 284: 14347–14358.

Chan SW, Lim CJ, Huang C, Chong YF, Gunaratne HJ, Hogue KA et al. (2011). WW domain-mediated interaction with Wbp2 is important for the oncogenic property of TAZ. Oncogene 30: 600–610.

Chawla A, Schwarz EJ, Dimaculangan DD, Lazar MA (1994). Peroxisome proliferator-activated receptor (PPAR) gamma: adipose-predominant expression and induction early in adipocyte differentiation. Endocrinology 135: 798–800.

Chen Y, Heiman ML (2001). Increased weight gain after ovariectomy is not a consequence of leptin resistance. Am J Physiol Endocrinol Metab 280: E315–E322.

Claessens F, Gewirth DT (2004). DNA recognition by nuclear receptors. Essays Biochem 40: 59–72.

Clevenger CV (2003). Nuclear localization and function of polypeptide ligands and their receptors: a new paradigm for hormone specificity within the mammary gland? Breast Cancer Res 5: 181–187.

Fu H, Subramanian RR, Masters SC (2000). 14-3-3 proteins: structure, function, and regulation. Annu Rev Pharmacol Toxicol 40: 617–647.

Harada S, Rodan GA (2003). Control of osteoblast function and regulation of bone mass. Nature 423: 349–355.

Hong JH, Yaffe MB (2006). TAZ: a beta-catenin-like molecule that regulates mesenchymal stem cell differentiation. Cell Cycle 5: 176–179.

Hong JH, Hwang ES, McManus MT, Amsterdam A, Tian Y, Kalmukova R et al. (2005). TAZ, a transcriptional modulator of mesenchymal stem cell differentiation. Science 309: 1074–1078.

Ito Y (2004). Oncogenic potential of the RUNX gene family: 'overview. Oncogene 23: 4198–4208.

Jans DA (1994). Nuclear signaling pathways for polypeptide ligands and their membrane receptors? Faseb J 8: 841–847.

Jeong H, Bae S, An SY, Byun MR, Hwang JH, Yaffe MB et al. (2010). TAZ as a novel enhancer of MyoD-mediated myogenic differentiation. Faseb J 24: 3310–3320.

Kanai F, Marignani PA, Sarbassova D, Yagi R, Hall RA, Donowitz M et al. (2000). TAZ: a novel transcriptional co-activator regulated by interactions with 14-3-3 and PDZ domain proteins. EMBO J 19: 6778–6791.

Kim M-S, Park J-S, Jang S-M, Lee BH, Ahn S-H AJH et al. (2011). Determination of a dipeptidyl peptidase IV agonist, [beta]-aminoacyl containing thiazolidine derivatives (KR-66223) in rat plasma by liquid chromatography-tandem mass spectrometry. J Pharm Biomed Anal 55: 1083–1088.

Komori T, Yagi H, Nomura S, Yamaguchi A, Sasaki K, Deguchi K et al. (1997). Targeted disruption of Cbfa1 results in a complete lack of bone formation owing to maturational arrest of osteoblasts. Cell 89: 755–764.

Kuroda R, Cutbush S, Neidle S, Leung OT (1985). Structural studies on some tamoxifen derivatives. J Med Chem 28: 1497–1503.

Lai D, Ho KC, Hao Y, Yang X (2011). Taxol resistance in breast cancer cells is mediated by the hippo pathway component TAZ and its downstream transcriptional targets Cyr61 and CTGF. Cancer Res 71: 2728–2738.

Lei QY, Zhang H, Zhao B, Zha ZY, Bai F, Pei XH et al. (2008). TAZ promotes cell proliferation and epithelial-mesenchymal transition and is inhibited by the hippo pathway. Mol Cell Biol 28: 2426–2436.

Lu PJ, Zhou XZ, Shen M, Lu KP (1999). Function of WW domains as phosphoserine- or phosphothreonine-binding modules. Science 283: 1325–1328.

MacLean HE, Warne GL, Zajac JD (1997). Localization of functional domains in the androgen receptor. J Steroid Biochem Mol Biol 62: 233–242.

Murakami M, Nakagawa M, Olson EN, Nakagawa O (2005). A WW domain protein TAZ is a critical coactivator for TBX5, a transcription factor implicated in Holt-Oram syndrome. Proc Natl Acad Sci USA 102: 18034–18039.

Nishikawa M, Akatsu T, Katayama Y, Yasutomo Y, Kado S, Kugal N et al. (1996). Bisphosphonates act on osteoblastic cells and inhibit osteoclast formation in mouse marrow cultures. Bone 18: 9–14.

Orwoll E, Ettinger M, Weiss S, Miller P, Kendler D, Graham J et al. (2000). Alendronate for the treatment of osteoporosis in men. N Engl J Med 343: 604–610.

Otto F, Thornell AP, Crompton T, Denzel A, Gilmour KC, Rosewell IR et al. (1997). Cbfa1, a candidate gene for cleidocranial dysplasia syndrome, is essential for osteoblast differentiation and bone development. Cell 89: 765–771.

Park KS, Whitsett JA, Di Palma T, Hong JH, Yaffe MB, Zannini M (2004). TAZ interacts with TTF-1 and regulates expression of surfactant protein-C. J Biol Chem 279: 17384–17390.

Ray S, Tandon A, Dwivedy I, Wilson SR, O'Neil JP, Katzenellenbogen JA (1994). An X-ray crystallographic study of the nonsteroidal contraceptive agent centchroman. J Med Chem 37: 696–700.

Rosen ED, Sarraf P, Troy AE, Bradwin G, Moore K, Milstone DS *et al.* (1999). PPAR gamma is required for the differentiation of adipose tissue in vivo and in vitro. Mol Cell 4: 611–617.

Ross SE, Hemati N, Longo KA, Bennett CN, Lucas PC, Erickson RL *et al.* (2000). Inhibition of adipogenesis by Wnt signaling. Science 289: 950–953.

Saag KG, Emkey R, Schnitzer TJ, Brown JP, Hawkins F, Goemaere S *et al.* (1998). Alendronate for the prevention and treatment of glucocorticoid-induced osteoporosis. Glucocorticoid-Induced Osteoporosis Intervention Study Group. N Engl J Med 339: 292–299.

Sahni M, Guenther HL, Fleisch H, Collin P, Martin TJ (1993). Bisphosphonates act on rat bone resorption through the mediation of osteoblasts. J Clin Invest 91: 2004–2011.

Shiau AK, Barstad D, Loria PM, Cheng L, Kushner PJ, Agard DA *et al.* (1998). The structural basis of estrogen receptor/coactivator recognition and the antagonism of this interaction by tamoxifen. Cell 95: 927–937.

Smith CL, O'Malley BW (2004). Coregulator function: a key to understanding tissue specificity of selective receptor modulators. Endocr Rev 25: 45–71.

Vitte C, Fleisch H, Guenther HL (1996). Bisphosphonates induce osteoblasts to secrete an inhibitor of osteoclast-mediated resorption. Endocrinology 137: 2324–2333.

Wang K, Degerny C, Xu M, Yang XJ (2009). YAP, TAZ, and Yorkie: a conserved family of signal-responsive transcriptional coregulators in animal development and human disease. Biochem Cell Biol 87: 77–91.

Wang CZ, Chen SM, Chen CH, Wang CK, Wang GJ, Chang JK *et al.* (2010). The effect of the local delivery of alendronate on human adipose-derived stem cell-based bone regeneration. Biomaterials 31: 8674–8683.

Watts NB, Diab DL (2010). Long-term use of bisphosphonates in osteoporosis. J Clin Endocrinol Metab 95: 1555–1565.

Wezeman FH, Emanuele MA, Moskal SF, Steiner J, Lapaglia N (2000). Alendronate administration and skeletal response during chronic alcohol intake in the adolescent male rat. J Bone Miner Res 15: 2033–2041.

Won HY, Lee J-A, Park ZS, Song JS, Kim HY, Jang S-M *et al.* (2011). Prominent Bone Loss Mediated by RANKL and IL-17 Produced by CD4+ T Cells in TallyHo/JngJ Mice. PLoS ONE 6: e18168.

Yoo SE, Kim SK, Lee SH, Yi KY, Lee DW (1999). A comparative molecular field analysis and molecular modelling studies on pyridylimidazole type of angiotensin II antagonists. Bioorg Med Chem 7: 2971–2976.

Zhang H, Liu CY, Zha ZY, Zhao B, Yao J, Zhao S *et al.* (2009). TEAD transcription factors mediate the function of TAZ in cell growth and epithelial-mesenchymal transition. J Biol Chem 284: 13355–13362.

Zhou Z, Hao Y, Liu N, Raptis L, Tsao MS, Yang X (2011). TAZ is a novel oncogene in non-small cell lung cancer. Oncogene 30: 2181–2186.